

International Journal of Modern Physics: Conference Series  
 © World Scientific Publishing Company

## Measurement of $^{230}\text{Pa}$ and $^{186}\text{Re}$ production cross sections induced by deuterons at ARRONAX facility

Charlotte DUCHEMIN, Arnaud GUERTIN, Vincent METIVIER

*Laboratoire SUBATECH, Ecole des Mines de Nantes, Université de Nantes, CNRS/IN2P3  
 4, rue Alfred Kastler, La Chantreterie  
 Nantes, 44307, France  
 Charlotte.Duchemin@subatech.in2p3.fr*

Ferid HADDAD, Nathalie MICHEL

*Laboratoire SUBATECH, Ecole des Mines de Nantes, Université de Nantes, CNRS/IN2P3  
 4, rue Alfred Kastler, La Chantreterie  
 Nantes, 44307, France  
 GIP Arronax, 1 rue Aronnax, Saint-Herblain, 44817, France*

Received Day Month Year

Revised Day Month Year

A dedicated program has been launched on production of innovative radionuclides for PET imaging and for  $\beta$ - and  $\alpha$  targeted radiotherapy using proton or  $\alpha$  particles at the ARRONAX cyclotron. Since the accelerator is also able to deliver deuteron beams up to 35 MeV, we have reconsidered the possibility to use them to produce medical isotopes. Two isotopes dedicated to targeted therapy have been considered :  $^{226}\text{Th}$ , a decay product of  $^{230}\text{Pa}$ , and  $^{186}\text{Re}$ . The production cross sections of  $^{230}\text{Pa}$  and  $^{186}\text{Re}$  have been determined using deuteron as projectile, as well as those of their contaminants created during the irradiation, by the stacked-foil technique. Experimental values have been quantified using a referenced cross section. The measured cross sections have been used to determine expected production yields and compared with the calculated values obtained using the Talys code with default parameters.

*Keywords:* production cross section; stacked-foil technique; Talys code; targeted radionuclide therapy; ARRONAX cyclotron

PACS numbers: 11.25.Hf, 123.1K

### 1. Introduction

The targeted radionuclide therapy<sup>1</sup> is one modality to treat cancer which consists in binding a radioactive isotope to a vector in order to target and then to destroy tumor cells. The choice of the isotope to be used depends on the characteristics of the targeted tumor :  $\alpha$  emitters will be well suited for microscopic disease whereas  $\beta$ - emitter will be used for millimeter tumor. Many isotopes are considered for such application. Among them,  $^{226}\text{Th}$  and  $^{186}\text{Re}$ , which may be advantageously produced using deuteron as projectile.  $^{226}\text{Th}$  ( $T_{1/2} = 31$  min), is an  $\alpha$  emitter which has been

## 2 Authors' Names

found a greater potential for leukemia therapies<sup>2</sup> than  $^{213}\text{Bi}$ . Indeed, the  $^{226}\text{Th}$  decay produces a cascade of four  $\alpha$  particles with a cumulated energy of 27.7 MeV. An additional interest is the possibility to use a radionuclide generator system  $^{230}\text{U}/^{226}\text{Th}$ .  $^{230}\text{U}$  ( $T_{1/2} = 21$  days) could be produced directly via  $^{231}\text{Pa}(p,2n)^{230}\text{U}$ , and indirectly via  $^{230}\text{Pa}$  ( $T_{1/2} = 17.4$  days) using proton or deuteron beams through  $^{232}\text{Th}(p,3n)^{230}\text{Pa} \rightarrow ^{230}\text{U}$ ,  $^{232}\text{Th}(d,4n)^{230}\text{Pa} \rightarrow ^{230}\text{U}$ . Twelve data sets are published concerning the  $^{230}\text{Pa}$  cross section induced by proton<sup>3</sup>, only one by deuteron<sup>4</sup>. A new set of data has been obtained in this study. Production yield have been determined from these data and compared with that of other production routes in order to determine the best one for  $^{230}\text{U}$  production.  $^{186}\text{Re}$  ( $T_{1/2} = 3.7$  days), is a  $\beta$ -emitter which has been used in clinical trials for palliation of painful bone metastases resulting from prostate and breast cancer<sup>5</sup>. Several cross section measurements have been made, since 1966, using proton or deuteron as projectile on a tungsten target<sup>3</sup>. Previous data show that deuteron as projectile is more interesting than proton, since it gives cross section values five times higher. As there are some disagreements between the existing series, this study aims to get additional data to better constrain the experimental trend. In both cases, our new sets determined via the stacked-foil technique<sup>6</sup> are compared with the existing experimental data and with Talys<sup>7</sup> code calculations made using default parameters.

## 2. Set-up and Data Measurements

Several stacks of natural tungsten and thorium have been irradiated at the AR-RONAX cyclotron<sup>8</sup>, in the AX hall devoted to experiments in physics, radiolysis and radiobiology. The stacks were placed in air, on an irradiation station called Nice-III. The beam line is closed using a kapton foil (75  $\mu\text{m}$ ) and the stack was located about 7 cm away. Taking into account the threshold at 16 MeV for  $^{230}\text{Pa}$ , two energy beams have been used for the  $^{230}\text{Pa}$  experiments, 30 and 22 MeV. For the determination of  $^{186}\text{Re}$  cross section, which energy threshold is low (3.6 MeV), deuteron beams at 16.4 MeV have been used. One high energy data point, around 22 MeV, has been obtained by putting a tungsten foil at the end of one thorium stack irradiated at 30 MeV. All foils were purchased from Goodfellow<sup>®</sup> (France) with high purity ( $\geq 99\%$ ). Each thin foil has been weighed before irradiation using an accurate scale ( $\pm 10^{-5}\text{g}$ ) and scanned, to determine the thickness precisely. Titanium monitor foils have been placed behind each target foil, to record the particle flux along the stack through the  $^{nat}\text{Ti}(d,x)^{48}\text{V}$  reaction, as suggested by IAEA<sup>9</sup>. In each foil, the  $^{48}\text{V}$  activity value has been determined after the complete decay of  $^{48}\text{Sc}$  ( $T_{1/2} = 43.67$  h). Nuclear data<sup>3</sup> associated to  $^{48}\text{V}$  are summarized in table 1. In addition to monitor foils, a Faraday cup was placed after the stack to collect charges and control the intensity during the irradiation. The incident beam energy was fixed by the setting parameters of the cyclotron. The energy through each thin foil was determined in the middle of the foil using the SRIM software<sup>10</sup>. Energy losses in the kapton foil and air were taken into account. Typical irradiations were carried

Table 1. Vanadium-48 half-life and main  $\gamma$  rays

Radioisotope	$T_{1/2}$ (days)	$E_\gamma$ (keV)	$I_\gamma$ (%)
$^{48}\text{V}$	15.9735(25)	944.104	7.870(7)
		983.517	99.98(4)
		1312.096	98.2(3)

out with about 100 nA for 30 minutes. Each target foil was separated from the stack and, after some cooling time, counting measurements were performed using a high purity germanium detector with low-background lead and copper shield from Canberra (France). Gamma spectra were recorded in a suitable geometry previously calibrated with standard  $^{57,60}\text{Co}$  and  $^{152}\text{Eu}$   $\gamma$  sources. The activity values of the produced radionuclides were derived from the spectra and the nuclear decay data<sup>11</sup> given in table 2, using the Fitzpeak spectroscopy software<sup>12</sup>. The dead time during the counting was always kept below 10% in order to reduce the effect of sum peaks.

Table 2. Produced radioisotope parameters from natural thorium and tungsten targets

Radioisotope	$T_{1/2}$ (days)	$E_\gamma$ (keV)	$I_\gamma$ (%)	Contributing reactions	$E_{threshold}$ (MeV)
$^{230}\text{Pa}$	17.4 (5)	951.95	29.1 (14)	$^{232}\text{Th}(\text{d},4\text{n})$	16.013
$^{232}\text{Pa}$	1.31 (2)	969.315	41.6 (19)	$^{232}\text{Th}(\text{d},2\text{n})$	3.537
$^{233}\text{Pa}$	26.967 (2)	312.17	38.6 (4)	$^{232}\text{Th}(\text{d},\text{n}) + (\text{d},\text{p})$ decay	0.000
				$^{232}\text{Th}(\text{d},\text{p})$ decay	0.000
$^{186}\text{Re}$	3.7183 (11)	137.157	9.42 (6)	$^{186}\text{W}(\text{d},2\text{n})$	3.626
$^{183}\text{Re}$	70.0 (11)	162.3219	23.3 (4)	$^{182}\text{W}(\text{d},\text{n})$	0.000
		208.8057	2.95 (5)	$^{183}\text{W}(\text{d},2\text{n})$	3.602
		292.7238	3.05 (16)	$^{184}\text{W}(\text{d},3\text{n})$	11.095
				$^{186}\text{W}(\text{d},5\text{n})$	24.180

Production cross section values can be determined from the activation formula (1) with the appropriate projectile flux.

$$\sigma = \frac{Act.A}{\Phi.N_a.\rho.e_f.(1 - e^{-\lambda.t})} \quad (1)$$

In this equation, the production cross section  $\sigma$  of a radioisotope depends on its measured activity ( $Act$ ), its decay constant ( $\lambda$ ), the target thickness ( $e_f$ ), its atomic number ( $A$ ), its density ( $\rho$ ), the irradiation duration ( $t$ ) and the projectile flux ( $\Phi$ ). In our experiment, each target foil received the same projectile flux as the following monitor foil. It is then easier to use the relative equation (2) in which the knowledge of the projectile flux is no longer necessary. In this equation, the prime parameters are associated to  $^{48}\text{V}$  monitor while the others relate to the Pa or Re isotopes, depending on the experiment.

$$\sigma = \sigma' \cdot \frac{Act.A.\rho'.e'_f.(1 - e^{-\lambda'.t})}{Act'.A'.\rho.e_f.(1 - e^{-\lambda.t})} \quad (2)$$

To determine the activity associated to each radionuclide of interest, all the target and monitor foils were counted twice with an interval of 2 weeks and during more than 24 hours. The cross section uncertainty is estimated with a propagation error calculation. Since all the parameters of equation (2) are independent, the total error

is expressed as a quadratic sum. The main error sources come from the recommended cross section (around 12%),  $^{230,232,233}\text{Pa}$  and  $^{186,187}\text{Re}$  activities (up to 12%),  $^{48}\text{V}$  activity (less than 2%) and thickness uncertainty (around 1%). The contribution of the irradiation time uncertainty is not significant and has been neglected.

### 3. Results

#### 3.1. Production of protactinium radionuclides

The irradiation of a thorium foil by a deuteron beam produces many residues through nuclear and fission reactions. As the specific activity of the final product is directly related to the isotopes of the element of interest, we have optimized our experiment to be able to measure them accurately. For that purpose, the first gamma spectra was acquired 2 days after the end of bombardment to get  $^{232}\text{Pa}$ , which has a half-life of only 1.3 days. In this paper, we only present data for  $^{230,232,233}\text{Pa}$  (all the nuclear parameters used are summarized in table 2), but data on fission residues have been also collected.

##### 3.1.1. Production of $^{230}\text{Pa}$

In the measured spectrum, we used the 951 keV  $\gamma$  line to determine the  $^{230}\text{Pa}$  activity value. Several other  $^{230}\text{Pa}$   $\gamma$  lines have been also identified between 397 and 1027 keV with branching ratios higher than 1%. Results from these lines were consistent, giving us confidence in our results. Using the second counting, we have verified that the line used was not fed by the decay of another isotope or a fission fragment product, and that the measured activity was consistent with the first one. The  $^{230}\text{Pa}$  production cross section as a function of the deuteron energy is plotted in figure 1.

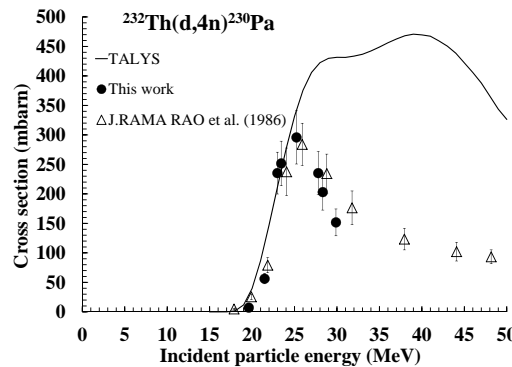


Fig. 1. Production cross section of  $^{232}\text{Th}(d,4n)^{230}\text{Pa}$

Our data points are presented as full circles whereas data from J.Rama Rao *et al.*<sup>4</sup> are plotted as empty triangles. Talys calculation values, performed using default parameters, are plotted as a solid line. Our new data set is consistent with the energy threshold associated to  $^{232}\text{Th}(d,4n)^{230}\text{Pa}$  and shows a

maximum of 296 mbarn at 25.2 MeV. Compared to the existing data from Ref. 4, the shape of our data set and the maximum value of the cross section are in good agreement. The Talys code calculation shows that neither the shape nor the maximum value of the cross section is reproduced. The  $\gamma$  spectra show that a lot of residues are produced coming from fission. Since Talys is also able to calculate their contribution, a comparison including all our data is underway.

### 3.1.2. Production of $^{232}\text{Pa}$

$^{232}\text{Pa}$  ( $T_{1/2} = 1.31$  d) emits a lot of detectable  $\gamma$  lines. In their work, J.Rama Rao *et al.*<sup>4</sup> choose to use the 894 keV  $\gamma$  line (22%). In our case, looking at the second counting when  $^{232}\text{Pa}$  has totally disappeared, a peak at this energy is still present which, we found, is coming from a sum peak between Pb X-ray (75 keV) from our shielding and  $^{136}\text{Cs}$   $\gamma$  line (819 keV), a fission fragment produced during the irradiation. We have preferred to use the 969 keV  $\gamma$  line with a higher branching ratio, 42.3% (table 2) subtracting the contribution of  $^{228}\text{Ac}$  ( $E = 969$  keV,  $I = 15.8\%$ ). The  $^{232}\text{Pa}$  cross section is represented in figure 2. Due to the  $^{230}\text{Pa}$

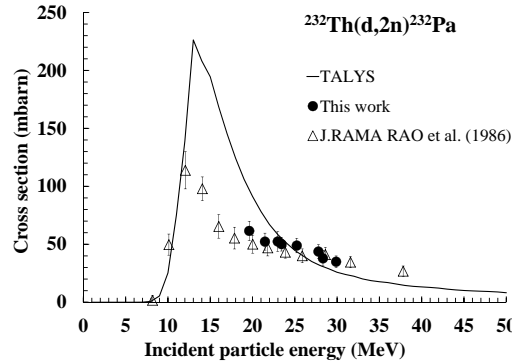


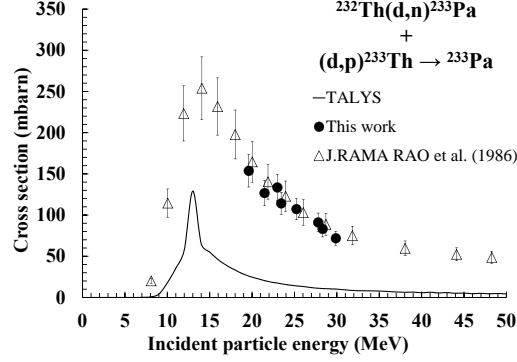
Fig. 2. Production cross section of  $^{232}\text{Th}(d,2n)^{232}\text{Pa}$

energy range of interest, we only have data points in the tail of the cross section curve. The trend is consistent with the existing data set from Ref. 4. Our values are slightly higher, mainly due to the different  $\gamma$  line used and the nuclear decay data updating. In fact, since 1986, the 894 keV  $\gamma$  line branching ratio used by Ref. 4 decreased from 22%<sup>4</sup> to 19,8%<sup>11</sup>. Talys results using default parameters are not in agreement with data even if the shape can be considered as not too bad.

### 3.1.3. Cumulative production of $^{233}\text{Pa}$

$^{233}\text{Pa}$  is produced directly through  $^{232}\text{Th}(d,n)$  but also indirectly by the decay of  $^{233}\text{Th}$  which is obtained via  $^{232}\text{Th}(d,p)$ . Since  $^{233}\text{Th}$  has a short half life ( $T_{1/2} = 21$  min), we were only able to measure the  $^{233}\text{Pa}$  cumulative cross section. These values compared to Ref. 4 and Talys are presented in figure 3. To follow the decay of  $^{233}\text{Pa}$  ( $T_{1/2} = 26.967$  d), we used the 312 keV  $\gamma$  line. Its high branching

6 Authors' Names

Fig. 3. Cumulative production cross section of  $^{233}\text{Pa}$ 

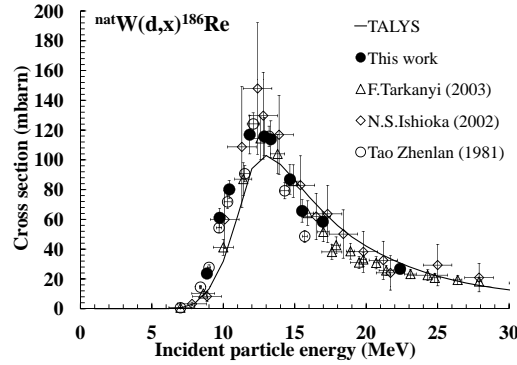
ratio (table 2) leads to a small uncertainty associated to the activity value (around 2.7%). Our data are very similar to those of Ref. 4. The small difference can be accounted by the branching ratio they used ( $I = 37\%$ ) which is lower than the current recommended value ( $I = 38.6\%$ ) listed in the databases<sup>3,11</sup>. The Talys results underestimate the amplitude and the peak width is poorly reproduced.

### 3.2. Production of rhenium radionuclides

In this second part, we have focused on the  $^{186}\text{Re}$  production cross sections induced by deuteron on a natural tungsten target. All the contaminants produced during this experiment have been measured.  $^{183}\text{Re}$  production cross section is also presented in this document. Indeed, due to its long half life ( $T_{1/2} = 70$  d),  $^{183}\text{Re}$  strongly affects the specific activity of the final product.

#### 3.2.1. Production of $^{186}\text{Re}$

The  $^{186}\text{Re}$  radionuclide has a half-life of  $T_{1/2} = 3.7183$  days and decreases at 92.53% by  $\beta^-$  to  $^{186}\text{Os}$  (stable) and at 7.47% by EC to  $^{186}\text{W}$  (stable). Its gamma line,

Fig. 4. Production cross section of  $^{nat}\text{W}(d,xn)^{186}\text{Re}$ 

$E_\gamma = 137.157$  keV ( $I = 9.47\%$ ), coming from the  $\beta^-$  decay, is used to measure the activity. In  $^{nat}\text{W}$ ,  $^{186}\text{Re}$  can only come from the  $^{186}\text{W}$ , the second most abundant isotope (28.6%). Our new data set is presented in figure 4 as full circles. This results

are very close to the Ref. 13 serie in the range 7 to 12 MeV and follows the Ref. 14 trend up to 17 MeV. Only Ref. 14 and Ref. 15 have contributed with higher energy beams and our result at 22 MeV is in agreement with their values. In this case, the Talys code gives satisfactory results, even if the shape is slightly smaller below 12 MeV.

### 3.2.2. Production of $^{183}\text{Re}$

The decay of the  $^{183}\text{Re}$  contaminant is followed by three main gamma radiations presented in table 2. It can be produced by four of the tungsten isotopes constituting the natural target. Our results are plotted in figure 5 with three other data sets.

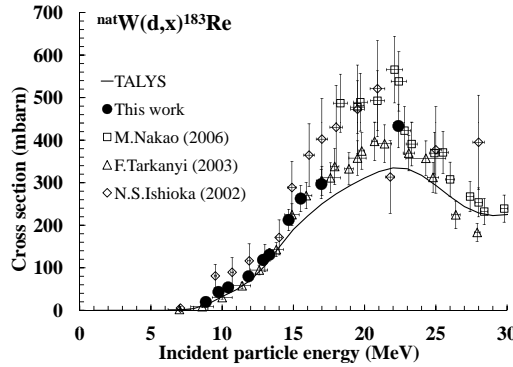


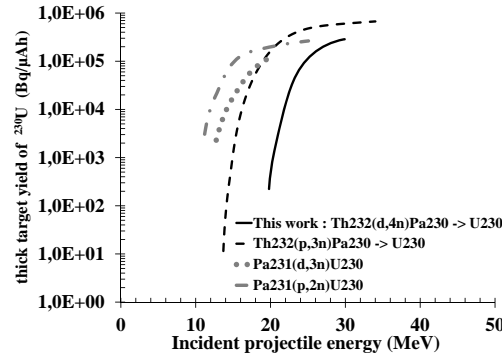
Fig. 5. Production cross section of  $^{nat}\text{W}(\text{d},\text{xn})^{183}\text{Re}$

These data show that the maximum cross section is around 20 MeV but with a different magnitude depending on the series. Our new values are coherent with the trend of Ref. 14 up to 17 MeV and around 22 MeV. New results above 17 MeV are needed to better discriminate between the different data sets previously published. Talys gives good results below 15 MeV and above 25 MeV. Between these two energies, the different experiments give values 16% to 35% higher than Talys.

## 4. Conclusion

In this work, new data sets concerning production cross sections induced by deuterons have been obtained. Presented values are in good agreement with the few existing data. In thorium, small differences were identified as coming from the recommended nuclear data change. Regarding to  $^{230}\text{Pa}$ , we have been able to calculate  $^{230}\text{U}$  thick target yield. This value has been compared with the other direct and indirect production routes<sup>17</sup> (Fig. 6). Whatever the production route, direct or indirect, proton beams always give higher  $^{230}\text{U}$  production values than deuteron beams. Both routes using protons are in the same order of magnitude. In one hand,  $^{232}\text{Th}$  target is easier to obtain and handle than  $^{231}\text{Pa}$ . In the other hand, by using  $^{232}\text{Th}$  target,  $^{230}\text{U}$  is indirectly produced via the  $^{230}\text{Pa}$  decay. This means that the  $^{230}\text{U}$  activity is obtained by eluting a  $^{230}\text{Pa}/^{230}\text{U}$  generator.

8 Authors' Names

Fig. 6.  $^{230}\text{U}$  thick target yield through different production routes

In the case of  $^{186}\text{Re}$ , the production cross section shows a maximum of 120 mbarn around 12 MeV. Using proton as projectile, the maximum value is 23.3 mbarn at 9 MeV (Ref. 9). The deuteron production route is clearly the best choice. All the contaminants created during irradiation were measured since a good optimization process is supposed to find the best compromise between production yield and purity of the final product. Comparisons with the Talys code have been performed using the default parameters. Differences have been found in the case of  $^{232}\text{Th}$  target. The fission products will be quantified in our experiments in order to better constrain the code calculation.

### Acknowledgments

The ARRONAX cyclotron is a project promoted by the Regional Council of Pays de la Loire financed by local authorities, the French government and the European Union. This work has been, in part, supported by a grant from the French National Agency for Research called "Investissements d'Avenir", Equipex Arronax-Plus n°ANR-11-EQPX-0004.

### References

1. A.Morgenstern, *8th Nuclear Science Training Course with Nuclides.net* (2006)
2. C.Friesen *et al.*, *Haematologica*, **94** [suppl.2]:329 (2009)
3. National Nuclear Data Center, BNL (USA)
4. J.Ramarao *et al.*, *Nucl.Phys.A* **448** 365-380 (1986)
5. H.Palmedo, J.K.Rockstroh *et al.*, *Radiology*, 221:256-260, (2001)
6. S.M.Qaim, *Appl. Radiat. Isot.* **Vol. 46**, 9, 955-960 (1995)
7. A.J.Koning *et al.*, "*TALYS-1.4*", *A nuclear reaction program* (December 28, 2011)
8. F.Haddad *et al.*, *Eur.J.Med.Mol.Imaging* 35:1377-1387 (2008)
9. IAEA, Nuclear Data Services, medical portal
10. J.Ziegler, *SRIM - The Stopping and Range of Ions in Matter* (2012)
11. The Lund/LBNL Nuclear Data Search
12. FitzPeak, Gamma Analysis and Calibration Software
13. Tao Zhenlan *et al.*, *Chinese J.of Nuclear Physics*, **Vol.3, Issue 3** p.242 (1981)
14. F.Tarkanyi *et al.*, *Nuc.Instr. and Meth. in Phys.Research B* **211** 319-330 (2003)
15. N.S.Ishioka *et al.*, *J.of Nuc.Science and Tech.Supply* **Vol.2** 1334 (2002)
16. M.Nakao *et al.*, *Nuc.Instr. and Meth. in Phys.Research A* **562** 785-788 (2006)
17. A. Morgenstern *et al.*, *Physical Review C* **80**, 054612 (2009)